

ORIGINAL ARTICLE

Open Access

# Subpopulation-proteomics reveal growth rate, but not cell cycling, as a major impact on protein composition in *Pseudomonas putida* KT2440

Sarah Lieder<sup>1</sup>, Michael Jahn<sup>2</sup>, Jana Seifert<sup>3,4</sup>, Martin von Bergen<sup>3,5,6</sup>, Susann Müller<sup>2</sup> and Ralf Takors<sup>1\*</sup>

## Abstract

Population heterogeneity occurring in industrial microbial bioprocesses is regarded as a putative effector causing performance loss in large scale. While the existence of subpopulations is a commonly accepted fact, their appearance and impact on process performance still remains rather unclear. During cell cycling, distinct subpopulations differing in cell division state and DNA content appear which contribute individually to the efficiency of the bioprocess. To identify stressed or impaired subpopulations, we analyzed the interplay of growth rate, cell cycle and phenotypic profile of subpopulations by using flow cytometry and cell sorting in conjunction with mass spectrometry based global proteomics. Adjusting distinct growth rates in chemostats with the model strain *Pseudomonas putida* KT2440, cells were differentiated by DNA content reflecting different cell cycle stages. The proteome of separated subpopulations at given growth rates was found to be highly similar, while different growth rates caused major changes of the protein inventory with respect to e.g. carbon storage, motility, lipid metabolism and the translational machinery. In conclusion, cells in various cell cycle stages at the same growth rate were found to have similar to identical proteome profiles showing no significant population heterogeneity on the proteome level. In contrast, the growth rate clearly determines the protein composition and therefore the metabolic strategy of the cells.

**Keywords:** Heterogeneity; Subpopulations; *Pseudomonas putida*; Proteome; Flow cytometry; Cell cycle

## Introduction

Commonly applied assumptions consider microbial populations in bioreactors as uniform, thus leveling individual properties of subpopulations to averages. However, it is increasingly accepted that clonal microbial cultures comprise individuals that are not identical, differing in terms of DNA content and cell physiology (Brehm-Stecher and Johnson 2004; Delvigne and Goffin 2013). Heterogeneity of clonal microbial cultures may result from several distinct sources, either from internal biological origins, such as mutations, cell cycle decisions and age distribution, or from 'external' technical factors (Avery 2006; Müller et al. 2010). Notably, external factors interact with biological properties, yielding the superimposition of both impacts in the population. Here, we shed light on the impact of

two key players in the origin of population heterogeneity, the growth rate and the cell cycle.

Traditionally, the cell cycle is suggested to play a role in the development of population heterogeneity within clonal populations (Müller et al. 2010). A short summary of the sequence of cell cycle phases can be found in Figure 1. The bacterial cell cycle was described for *Escherichia coli* comprising the B-Phase, which is defined as the time between division and start of replication, the replication phase (C-Phase), the pre-D-Phase (an interphase between the C- and D-Phase) and the division phase (D-Phase) (Cooper 1991; Müller and Babel 2003). Furthermore, under optimal growth conditions accelerated proliferation (also called 'multifork DNA-replication') can be monitored: new rounds of DNA replication may be initiated before a previous round is completed, putatively providing another source of heterogeneity (Bley 1990; Müller 2007).

\* Correspondence: takors@ibvt.uni-stuttgart.de

<sup>1</sup>Institute for Biochemical Engineering, University of Stuttgart, Allmandring 31, Stuttgart, Germany

Full list of author information is available at the end of the article

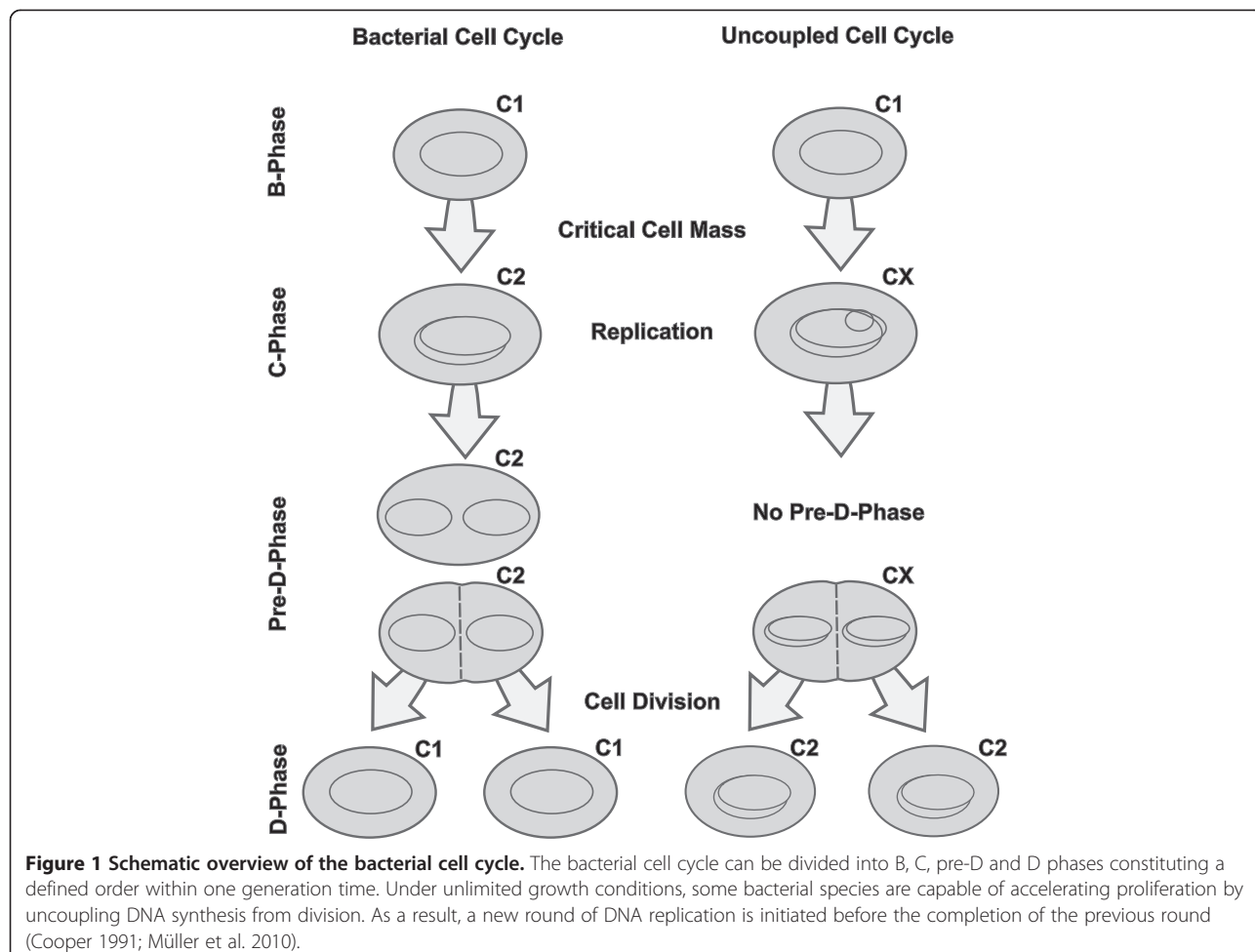


**Figure 1** Schematic overview of the bacterial cell cycle. The bacterial cell cycle can be divided into B, C, pre-D and D phases constituting a defined order within one generation time. Under unlimited growth conditions, some bacterial species are capable of accelerating proliferation by uncoupling DNA synthesis from division. As a result, a new round of DNA replication is initiated before the completion of the previous round (Cooper 1991; Müller et al. 2010).

It is suspected, that biosynthesis of biotechnological interesting compounds occurs in dependency of the cell cycle, e.g. only within the stochastic B- and pre-D-phases, when cells are neither replicating nor dividing (Müller et al. 2010). Ackermann et al. (1995) described for *Methylobacterium rhodesianum* that products like polyhydroxylalkanoates (PHAs) accumulate only when cells comprise a certain chromosome number. This phenomenon was found to occur at off-cell-cycling stages. In microbial biotechnology, heterogeneity caused by cell cycling may cause inefficiently producing subpopulations and could have significant impact on the overall process performance (Lencastre Fernandes et al. 2011). Here, we aim to investigate if the protein inventory of a cell, which is related to its metabolic activity, is dependent on cell cycle stages and how growth rates may influence both, protein composition and cell cycling.

*Pseudomonas putida* KT2440 was used as a model organism owing to its numerous qualities as an expression host, such as safety (Bagdasarian et al. 1981; Nakazawa and Yokota 1973), fast growth, a fully sequenced genome (Nelson et al. 2002) and high stress tolerance (Martins

Dos Santos et al. 2004). Together with simple nutrient demand, the potential to regenerate redox cofactors at a high rate (Blank et al. 2008) and its amenability to genetic manipulation, *P. putida* is an ideal host for heterologous gene expression (Meijnen et al. 2008). With the advance of genome-wide pathway modeling (Puchałka et al. 2008) and 'omics techniques, the way for systems-wide engineering strategies was paved to turn *P. putida* into a flexible cell factory chassis (Yuste et al. 2006). Consequently, *P. putida* is more and more explored and already successfully used for numerous industrial applications (Poblete-Castro et al. 2012; Puchałka et al. 2008).

In our study, we applied continuous cultivations under controlled growth conditions at defined growth rates. While (fed-) batch approaches are characterized by steadily changing environmental conditions such as media composition, steady-state modes of a chemostat, where cells are cultivated with a pre-installed growth rate, are defined by environmental conditions that remain unchanged (Carlquist et al. 2012). Notably, (fed-) batch cultures usually represent a mixture of cells growing with different speed as a consequence of changing environmental conditions (Unthan et al. 2014).

Investigating a wide spectrum of growth rates with chemostat cultivation and sampling at steady state conditions gave a specific and unmasked view on the influence of the growth rate on population characteristics. Features like DNA content of the cells, protein composition and adenylate energy charge measurements were included in the study. Additionally, subpopulations with different DNA content were sorted at growth rates  $0.1\text{ h}^{-1}$ ,  $0.2\text{ h}^{-1}$  and  $0.7\text{ h}^{-1}$  and analyzed for their proteome composition.

Summarizing, we investigated if cell cycling subpopulations at the same growth rate were independent and different from each other on the level of metabolic pathways, e.g. whether slow growing cells with longer cell cycling phases might specialize between proliferation and production phases. In addition, we wanted to clarify if cells invest into different protein species under rising growth rates.

## Materials and methods

### Bacterial strains and cultivation conditions

Chemicals were purchased from Fluka, St. Gallen, Switzerland. Experiments were performed with *P. putida* KT2440 (ATCC 47054) cells originating from a single colony stored in a working cell bank at  $-70^{\circ}\text{C}$ . Cells were cultivated in M12 minimal salt medium containing  $2.2\text{ g L}^{-1}$   $(\text{NH}_4)_2\text{SO}_4$ ,  $0.4\text{ g L}^{-1}$   $\text{MgSO}_4 \cdot 7\text{ H}_2\text{O}$ ,  $0.04\text{ g L}^{-1}$   $\text{CaCl}_2 \cdot 2\text{ H}_2\text{O}$ ,  $0.02\text{ g L}^{-1}$   $\text{NaCl}$ ,  $2\text{ g L}^{-1}$   $\text{KH}_2\text{PO}_4$  and trace elements ( $2\text{ mg L}^{-1}$   $\text{ZnSO}_4 \cdot 7\text{ H}_2\text{O}$ ,  $1\text{ mg L}^{-1}$   $\text{MnCl}_2 \cdot 4\text{ H}_2\text{O}$ ,  $15\text{ mg L}^{-1}$   $\text{Na}_3\text{-citrate} \cdot 2\text{ H}_2\text{O}$ ,  $1\text{ mg L}^{-1}$   $\text{CuSO}_4 \cdot 5\text{ H}_2\text{O}$ ,  $0.02\text{ mg L}^{-1}$   $\text{NiCl}_2 \cdot 6\text{ H}_2\text{O}$ ,  $0.03\text{ mg L}^{-1}$   $\text{NaMoO}_4 \cdot 2\text{ H}_2\text{O}$ ,  $0.3\text{ mg L}^{-1}$   $\text{H}_3\text{BO}_3$ ,  $10\text{ mg L}^{-1}$   $\text{FeSO}_4 \cdot 7\text{ H}_2\text{O}$ ).

A shake flask preculture (150 mL) was started from a minimal medium working cell bank (8.5 mL) with a glucose concentration of  $5\text{ g L}^{-1}$ . At mid-exponential growth phase, the preculture was used to inoculate the bioreactor (KLF 3.7 L, Ser. No. 10819, Bioengineering AG, Wald, Switzerland) to reach a final working volume of 1.5 L. Before inoculation, the cultivation conditions were set to  $30^{\circ}\text{C}$ , a stirrer speed of 700 rpm, a pressure of 0.5 bar and an aeration of  $2\text{ L min}^{-1}$  sterile filtered ambient air. The pH was set and maintained at pH 7 with 25% (v/v)  $\text{NH}_4\text{OH}$ . Exhaust gas composition (Blue Sense  $\text{CO}_2$  and  $\text{O}_2$ , (DCP-CO2 DCP-02, Blue Sense gas sensor GmbH, Herten, Germany), dissolved oxygen and pH in the liquid phase (Ingold, Mettler Toledo GmbH, Giessen, Germany) were monitored online. After glucose depletion, the batch cultivation was continued as a chemostat. At steady state conditions, the dilution rate equals the specific growth rate  $\mu$  in a chemostat set-up. Each dilution rate (and therefore growth rate) and environmental condition was kept for 5 residence times. The dilution rate was adjusted by feeding at a defined flow rate. Weight gain of the reactor was monitored and a harvest pump was started at a

weight gain of 10 g. Additionally, the dilution rate was checked manually by measuring the mass of the harvest outflow within a timespan of one hour before sampling. Steady state was evaluated online via exhaust air analysis. Chemostat cultivations were performed in three individual biological replicates.

### Determination of the adenylate energy charge

The adenylate energy charge (AEC) value mirrors the cellular energy status (Atkinson and Walton 1967) and can be assessed as follows: Biocatalytic reactions inside the cells were stopped with 35% (w/v)  $\text{HClO}_4$ . 4 mL biosuspension was taken directly into 1 mL of precooled ( $-20^{\circ}\text{C}$ )  $\text{HClO}_4$  solution on ice and mixed immediately (Theobald et al. 1997). The sample was shaken at  $4^{\circ}\text{C}$  for 15 min in an overhead rotation shaker. Afterwards, the solution was neutralized on ice by fast addition of 1 mL 1 M  $\text{K}_2\text{HPO}_4$  and 0.9 mL 5 M KOH (Buchholz et al. 2001). The neutral solution was centrifuged at  $4^{\circ}\text{C}$  and  $4,000\times g$  for 10 min to remove cell debris, precipitated protein and potassium perchlorate. The supernatant was kept at  $-20^{\circ}\text{C}$  for batch high pressure liquid chromatography (HPLC) measurements. At each sampling time, the biosuspension sample and a filtrated sample without cells was treated according to the above described procedure.

Nucleotide analysis was performed by reversed phase ion pair HPLC (Theobald et al. 1997). The HPLC system (Agilent Technologies, Waldbronn, Germany) consisted of an Agilent 1200 series autosampler, an Agilent 1200 series Binary Pump SL, an Agilent 1200 series thermostated column compartment, and an Agilent 1200 series diode array detector set at 260 and 340 nm. The nucleotides were separated and quantified on an RP-C-18 column that was combined with a guard column (Supelcosil LC-18-T; 15 cm  $\times$  4.6 mm, 3  $\mu\text{m}$  packing and Supelguard LC-18-T replacement cartridges, 2 cm; Supelco, Bellefonte, USA) at a flow rate of 1 ml/min. A gradient elution method (Cserjan-Puschmann et al. 1999) was adapted and performed with two mobile phases, buffer A (0.1 M  $\text{KH}_2\text{PO}_4$ /  $\text{K}_2\text{HPO}_4$ , with 4 mM tetrabutylammonium sulfate and 0.5% (v/v) methanol, pH 6.0) and (ii) solvent B (70% (v/v) buffer A and 30% (v/v) methanol, pH 7.2). The following gradient programs were implemented: 100% (v/v) buffer A from 0 min to 3.5 min, increased to 100% (v/v) B until 43.5 min, remaining at 100% (v/v) B until 51 min, decreased to 100% (v/v) A until 56 min and remaining at 100% (v/v) A until 66 min.

The AEC is calculated according to Atkinson and Walton (1967):

$$AEC = \frac{[\text{ATP}] + 0.5 \cdot [\text{ADP}]}{[\text{AMP}] + [\text{ADP}] + [\text{ATP}]} \quad (1)$$

### Sample preparation and staining for flow cytometry

Samples for flow cytometry were washed with PBS, re-suspended in cryo-protective solution (15% (v/v) glycerol in PBS according to Jahn et al. (2013)) and stored at -20°C.

Deep-frozen cell samples were thawed on ice and centrifuged for 2 min at 8,000×g and 4°C to remove the cryo-protective solution. The supernatant was discarded, the cells were resuspended in ice cold PBS and adjusted to an optical density of OD<sub>600nm</sub> = 0.05 in 2 mL volume. For DNA staining, the cells were centrifuged, taken up in 1 mL permeabilization buffer (0.1 M citric acid, 5 g L<sup>-1</sup> Tween 20), incubated for 10 min on ice, centrifuged again and the supernatant was removed. Finally, cells were resuspended in 2 mL ice cold staining buffer (0.68 μM DAPI, 0.1 M Na<sub>2</sub>HPO<sub>4</sub>), filtered through a Partec Cell-Trics mesh (Partec, Germany) with 30 μm pore size and stored on ice until analysis.

### Flow cytometry and cell sorting

Flow cytometry was performed using biological duplicates. For each biological replicate two technical replicates were investigated using a MoFlo cell sorter (Beckman-Coulter, USA) as described before (Jahn et al. 2013; Jehmllich et al. 2010). Forward scatter (FSC) and side scatter signals (SSC) were acquired using blue laser excitation (488 nm, 400 mW) and a bandpass filter of 488/10 nm together with a neutral density filter of 2.0 for emission. The DAPI fluorescence was recorded using a multi-line UV laser for excitation (333–365 nm, 100 mW) and a bandpass filter of 450 ± 30 nm for emission. The datasets were annotated according to the miFlowCyt standard (Lee et al. 2008) and are publicly available on the FlowRepository database (Spidlen et al. 2012). Cells were sorted at the most accurate mode (single cell, one drop) with a sorting speed of 4,000 s<sup>-1</sup> and a sample chamber cooled to 4°C. For cell sorting a total number of 5 × 10<sup>6</sup> cells per replicate were directly sorted on a filter well plate (LoProdyne™ membrane with 0.45 μm pore size, Nunc, Germany) and the residual buffer was constantly drawn off by an exhaust pump. After sorting, the filter membrane was washed three times with 200 μL PBS, air dried and stored at -20°C for further analysis.

### Identification of proteins by LC-MS-MS

For quantitative proteomics, the filter membrane was cut into smaller pieces and treated by trypsin for whole cell proteolytic digestion as described in Jahn et al. (2013). The obtained peptide solution was purified using the Zip-Tip protocol (Millipore, USA), dried in a vacuum concentrator at 30°C and finally taken up in 20 μL 0.1% (w/v) formic acid. The solution was separated by nano-ultra performance liquid chromatography and measured by an

LTQ Orbitrap XL (Thermo Fisher Scientific, Germany) as described in Jahn et al. (2013).

### Data analysis

Mass spectra were analyzed by MaxQuant v1.2.2.5 (Cox and Mann 2008) for protein identification and label-free quantification with the genome database of *P. putida* KT2440 and the settings given in Jahn et al. (2013). The label-free quantification (LFQ) values were used for further data analysis and can be found in the Additional file 1. The mean, standard deviation and relative quantity of replicates in relation to the reference population (RP,  $\mu = 0.2 \text{ h}^{-1}$ , mean of two biological replicates) was calculated. The RP was sorted in order to exclude influences of the sorting procedure on the proteomic content. Unsorted cells of the 0.2 h<sup>-1</sup> grown population were used as an unaffected control population (CP). Student's *t*-test was performed for significance testing ( $p < 0.05$ ) of single proteins. Proteins were annotated using COG (clusters of orthologous groups) (Tatusov et al. 1997) and clustered in two hierarchical levels of metabolic pathways ('metabolism', 'pathway'). Protein clusters were tested for significant changes using the R Bioconductor (www.bioconductor.org) packages GAGE (Luo et al. 2009) and GlobalTest (Goeman et al. 2006), setting  $p < 0.05$  and a relative fold change (FC) of 1.5 ( $\log_2 \text{FC} > 0.58$ ) as thresholds. Hierarchical groups were visualized using a color-coded circular treemap (Jahn et al. 2013).

### Results

Subpopulation dynamics of *P. putida* KT2440 were analyzed in a wide range from slow growth rates starting at  $\mu = 0.1 \text{ h}^{-1}$  to high growth rates of up to  $\mu = 0.7 \text{ h}^{-1}$ . At growth rates higher than  $\mu = 0.7 \text{ h}^{-1}$ , wash out of the culture was observed, meaning that the maximal growth rate was exceeded and cells could not reproduce fast enough to keep the population density constant. For this reason,  $\mu = 0.7 \text{ h}^{-1}$  was the highest growth rate investigated in this study. The physiological and the energetic state of the averaged cell population was analyzed by biomass/substrate yield ( $Y_{x/s}$ ), biomass specific substrate uptake rates ( $q_s$ ), and adenylate energy charge measurements (AEC), each measured at steady state growth conditions (Figure 2). Observed stable carbon dioxide emission rates served as the criterion to qualify the achievement of steady-state cultivation conditions.

The yield of biomass on glucose increased gradually by 10% from  $\mu = 0.1 \text{ h}^{-1}$  to  $\mu = 0.5 \text{ h}^{-1}$ . Further rise of the growth rate resulted in yield reductions, returning to the level at  $\mu = 0.1 \text{ h}^{-1}$  (-10%). The energetic capacity of the cells can be estimated via AEC, taking the relative contribution of all three phosphorylated forms of adenine into account. The AEC was found to be stable with

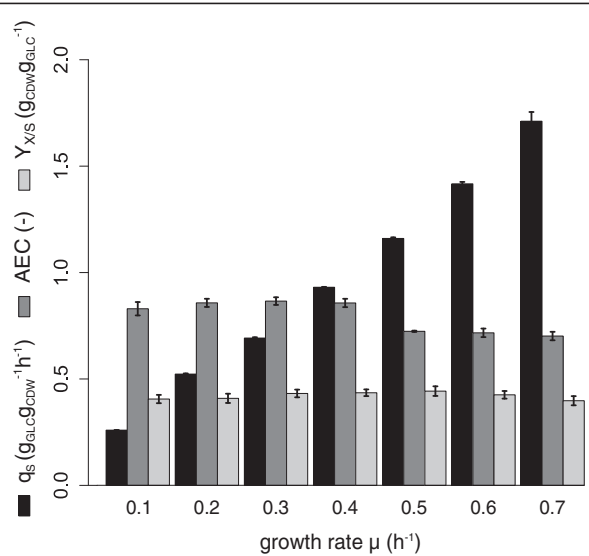


**Figure 2 Summary of the physiological state of the average population.** The specific glucose uptake rate ( $q_s$ ,  $\text{g}_{\text{GLC}} \text{g}_{\text{CDW}}^{-1} \text{h}^{-1}$ , black bars), the adenylate energy charge (AEC, dark grey bars) and the biomass yield ( $Y_{x/s}$ ,  $\text{g}_{\text{CDW}} \text{g}_{\text{GLC}}^{-1}$ , light grey bars) were measured at steady state conditions for different growth rates  $\mu$  ( $\text{h}^{-1}$ ). The growth rate was stepwise increased until a wash-out of the cells was monitored. Concentrations of cell dry weight (CDW), glucose (GLC) and the AEC were measured offline, sampling after 5 residence times of one specific growth rate ( $0.1 \leq \mu (\text{h}^{-1}) \leq 0.7$ ). Error bars show the standard deviation between three biological replicate cultivations.

increasing growth rate until  $\mu = 0.4 \text{ h}^{-1}$ . Further increasing the growth rate resulted in a reduction of the AEC level by  $\sim 18\%$  ( $p$ -value  $< 0.01$ ), which was almost the same at maximum growth, still staying in the range of expected physiological levels. The specific glucose uptake rate  $q_s$  was increasing linearly with increasing growth rate.

To be able to distinguish between subpopulations, flow cytometry was proven to be a suitable tool shedding light on the dynamics of single cells within a heterogeneous microbial population (Cooper 1991; Müller and Babel 2003; Shapiro 2000; Skarstad et al. 1985). Here, the DNA content was monitored via flow cytometry in addition to forward scattering (FSC) giving relative information about cell size (Müller and Nebe-Von-Caron 2010) (Figure 3). The dataset of the biological replicate can be found in the Additional file 2: Figure S1. The subpopulation analysis revealed that the major differential parameter was the alteration of DNA content as distinguished by flow cytometry. Three subpopulations could be identified in total: cells containing a single chromosome equivalent (C1), two chromosome equivalents (C2) and cells with more than two chromosome equivalents (Cx) (Figure 3). Population composition with respect to DNA content varied clearly as a function of growth rates. At  $\mu = 0.1 \text{ h}^{-1}$ ,  $82.0 \pm 0.3\%$  of cells contained a single chromosome equivalent, while only  $18.0 \pm 0.2\%$  contained a double chromosome equivalent content. No Cx subpopulation could be detected. On the contrary, at the high growth rate of  $\mu = 0.7 \text{ h}^{-1}$  only  $1.4 \pm 0.8\%$  of cells belonged to the C1 subpopulation,  $16.1 \pm 0.1\%$  of cells contained a double chromosome content and  $82.5 \pm 1.0\%$  more than double.

To investigate whether subpopulations with different DNA content show physiological differences as well, we sorted the cell population at three growth rates ( $0.1 \text{ h}^{-1}$ ,  $0.2 \text{ h}^{-1}$  and  $0.7 \text{ h}^{-1}$ ) into subpopulations containing single (C1), double (C2) or more than double chromosome content (Cx) aiming to analyze their proteome profile as the basis of their phenotype. In total, 677 unique proteins could be detected. 351 proteins were found in at

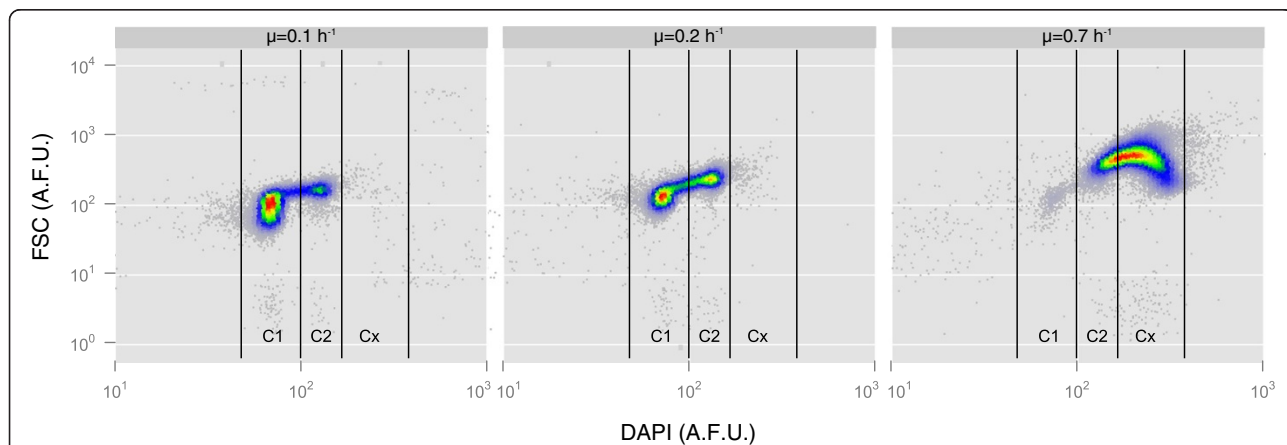


**Figure 3 Dot plots of DNA content (DAPI, in arbitrary fluorescence units (A.F.U.)) versus forward scatter (FSC, in A.F.U.) at different growth rates  $0.1 \text{ h}^{-1}$ ,  $0.2 \text{ h}^{-1}$  and  $0.7 \text{ h}^{-1}$ .** The dataset of the biological replicate can be found in the Additional file 2: Figure S1. Cells of *P. putida* KT2440 grown at steady state conditions in chemostats were stained with DAPI and analyzed by flow cytometry. The DNA content and the forward scatter increased with increasing growth rate. The indicated gates (C1, C2, Cx) were used for sorting  $5 \times 10^6$  cells per subpopulation for further mass spectrometric analysis.

least one replicate of all subpopulations and 245 proteins were found across all replicates. 707 different functions of 647 unique proteins were annotated using the database of clusters of orthologous groups (COG) (Tatusov et al. 1997) (Additional file 2: Figure S2). 95.2% of the non-sorted control population (CP) proteome could be found in the reference population (RP) proteome without significant changes, indicating only a small influence of cell sorting on protein recovery and confirming the quality of the analysis.

Significant changes in protein quantity were defined by exceeding a threshold of more than 1.5 fold change (FC) in combination with a *p*-value < 0.05 (Student's *t*-test). Changes in metabolic pathways were detected using GAGE and GlobalTest gene set analysis (Goeman et al. 2006; Luo et al. 2009) applying the same significance filter as for the individual proteins.

As a result, at any given growth rate, the proteomic patterns of the subpopulations did not differ significantly from each other (Figure 4a). When looking at single proteins, only three were detected that comprised significantly different levels between subpopulations at growth rate  $\mu = 0.1 \text{ h}^{-1}$  and  $\mu = 0.7 \text{ h}^{-1}$ , respectively. The abundance of cell division protein FtsZ was found to be 3.6 fold lower in subpopulation C1 in contrast to C2. FtsZ is a bacterial tubulin homologue self-assembling into a ring at mid-cell level and localizing the bacterial divisome machinery (Adams and Errington 2009; Weart et al. 2007). The two other proteins were the molecular chaperone GroEL (FC 1.7) and a P-47-like protein (PP\_2007, FC 2.4). Also at high growth rate of  $\mu = 0.7 \text{ h}^{-1}$ , only three proteins, the translocation protein TolB (FC 1.8), the NADH dehydrogenase subunit G (PP\_4124, FC 1.51) and a succinyl-diaminopimelate transaminase (PP\_1588, FC 0.26) showed significant differences between the subpopulations C2 and Cx. Surprisingly, no changes in metabolic pathways could be found between subpopulations at any given growth rate.

Comparing the subpopulations of different growth rates with RP, biologically significant differences were detectable as tested by gene set analysis (GAGE (Luo et al. 2009) and Globaltest (Goeman et al. 2006)) (Figure 4b and 4c). At  $\mu = 0.1 \text{ h}^{-1}$ , subpopulations C1 and C2 showed higher abundance of proteins related to 'cell motility', and proteins involved in 'cell cycle control, cell division and chromosome partitioning' (cell cycle) were additionally highly abundant in subpopulation C2. Apart from COG annotated pathways, several proteins connected to carbon storage were found to be significantly changed (Figure 5). Mirroring low  $q_s$  at slow growth compared to moderate growth, four main signaling proteins in chemotaxis (CheA, CheB, CheW, CheV) as well as 6 methyl accepting chemotaxis transducers were significantly increased. Furthermore, the low abundance of glycogen synthesis proteins (GlgA, Pgm) and the high abundance of glycogen

hydrolysis proteins (GlgX, GlgP) could be seen together with an increase of proteins involved in PHA production (PhaA, PhaC).

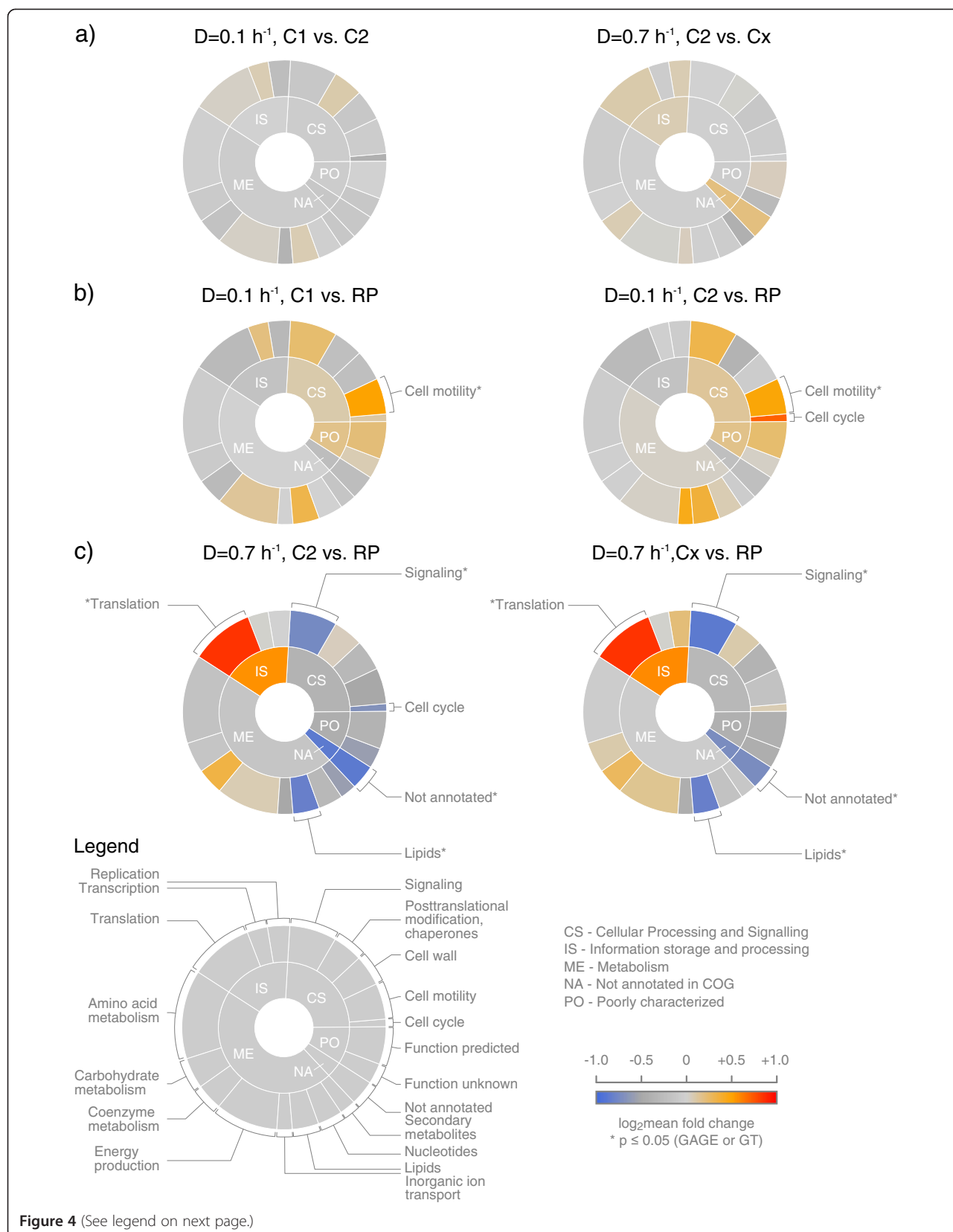
In contrast, subpopulations C2 and Cx of fast growing cells ( $\mu = 0.7 \text{ h}^{-1}$ ) revealed higher presence of proteins grouped in the pathway 'Translation, ribosomal structure and biogenesis' (Translation), while proteins of 'Signal transduction mechanisms' (Signaling) and 'Lipid transport and metabolism' (Lipids), were significantly underrepresented. The faster growth was reflected in proteins related to translation and therefore protein production. Here, 11 tRNA synthetases and 25 ribosomal proteins showed significantly higher abundance. In lipid metabolism, mostly enzymes of beta-oxidation were found in lower presence at fast growth (Figure 5). The supposed down regulation of the 'Cell Cycle' (C2 versus Cx) was mainly due to the single protein change of the poorly characterized PP\_3128.

In summary, the proteome of cells differing in DNA content but of identical growth rate was highly similar, whereas the proteome of cells cultivated at different growth rates was significantly diverging in particular pathways.

## Discussion

Considering the influence of different growth rates on the population, proteome analysis revealed that slow growth triggered starvation response, while fast growing cells displayed accelerated protein synthesis and alleviated stress physiology. In slowly growing cells, proteins connected to PHA synthesis and glycerol hydrolysis were amplified, indicating higher PHA carbon storage activity. Additionally, these cells showed protein patterns anticipating increased motility and chemotaxis response. Notably, low  $q_s$  values of slowly growing cells ( $\mu = 0.1 \text{ h}^{-1}$ ) were not reflected on the energetic state of the population. AEC values did not differ significantly between slow and moderate growth rates of  $0.1 \text{ h}^{-1}$  and  $0.4 \text{ h}^{-1}$ , respectively. Chemotaxis and cellular motility as a response to carbon-poor conditions are well-known phenomena in natural environments (Harshey 2003; Soutourina and Bertin 2003). Our observations in slowly growing cells are in agreement with findings of transcriptome studies in 'average populations' of other species. For instance, studies in *E. coli* showed higher expression of genes involved in motility at slower growth rates in direct comparison to faster growth conditions (Nahku et al. 2010) and studies in *Saccharomyces cerevisiae* showed significant amplification of carbon storage metabolism at slow growth (François and Parrou 2001).

Fast growing cells were obviously investing resources in proteins involved or related to the translation machinery. Multiple ribosomal proteins as well as tRNA synthetases were highly abundant fostering protein/biomass production (Figure 5). This finding is also in agreement



(See figure on previous page.)

**Figure 4 Circular treemaps visualizing differentially expressed functional protein categories.** Proteins detected by mass spectrometry were clustered according to their pathway annotation in COG covering two levels of specificity (Tatusov et al. 1997). The size of a sector is proportional to the number of proteins found in one specific pathway in relation to the total protein number. The color code represents the  $\log_2$  mean fold change ( $\log_2 FC$ ) of protein quantity in one pathway. The color blue codes for an underrepresentation, red for an overrepresentation of the proteins in a pathway compared to the reference population (RP,  $\mu = 0.2 \text{ h}^{-1}$ ). Pathways with a fold change in the range  $\log_2 FC < -0.58$  and  $\log_2 FC > 0.58$  are labeled with the respective pathway name. Pathways that were significantly changed using GAGE (Luo et al. 2009) and Globaltest (Goeman et al. 2006) gene set analysis are additionally marked (\*). **a.** Comparison of the subpopulations C1/C2 and C2/Cx at growth rates  $0.1 \text{ h}^{-1}$  and  $0.7 \text{ h}^{-1}$ , respectively. **b.** Comparison of the subpopulations C1 and C2 at  $\mu = 0.1 \text{ h}^{-1}$  with RP. **c.** Comparison of the subpopulations C2 and Cx at  $\mu = 0.7 \text{ h}^{-1}$  with RP.

with observations in eukaryotes like *S. cerevisiae* (Rebnegger et al. 2014) and prokaryotes such as *Salmonella typhimurium* (Schaechter et al. 1958). Additionally, proteins of typical carbon storage pathways, e.g. PHA synthesis, were less abundant in *P. putida* KT2440. Proteins of lipid biosynthesis, especially involved in beta oxidation were also lowered in fast growing cells compared to RP. This observation is in agreement with the lower abundance of the PHA synthesis proteins, as the beta oxidation provides precursors for this pathway (Aldor and Keasling 2003).

To our surprise, the almost 6.5-fold increase of the specific glucose uptake rate with increasing growth rate (Figure 2), was not mirrored by major changes

among proteins involved in carbohydrate and energy metabolism.

Notably, relative changes of protein quantity can be elucidated with the method applied here. Absolute changes per cell, dependent on the growth rate were not measured with the applied workflow, as it was first shown for the sum of proteins by Schaechter et al. (1958). Their pioneering studies described an exponential increase in protein, DNA and RNA contents and therefore, cell size with increasing growth rates (Bremer and Dennis 1996; Maaløe and Kjeldgaard 1966; Schaechter et al. 1958). In our study, the relative cell size estimation was acquired using FSC. In accordance to various other cell cycle analyses, the FSC increased with increasing growth rates (Donachie 1968; Hewitt et al. 1999; Neumeyer et al. 2013; Skarstad et al. 1983) (Figure 3). Following the rational of Schaechter et al. (1958), this phenomenon reflects increasing protein contents per cell. We presume that the increased amount of cellular glucose uptake is proportional to the elevated production of proteins, thus increasing absolute protein quantity but leaving relative quantity unchanged.

Studying the putative impact of growth rate and cell cycle stage on the functional diversity of a population, the growth rate is obviously a major determinant for cellular protein composition, as found in our chemostat studies. Growth and cell cycle were clearly linked, but subpopulations showing different DNA content showed only small differences in cellular physiology at the same growth rate. The detection of FtsZ in a significant higher abundance in the C2 subpopulation, which is preparing for division after finishing replication, is in agreement with its assigned function as a proposed diffusible factor (Teather et al. 1974) initiating cell division (Chien et al. 2012). Despite this cell cycle related finding, subpopulations showed almost identical protein patterns irrespective of cell sizes, anticipated protein mass (Lindmo 1982; Rønning et al. 1979) and DNA content.

Surprisingly, no signs for a specialization of cells in different cell stages for e.g. carbon storage or protein production/growth could be observed that could support the hypothesis of shared tasks of subpopulations in B- and pre-D/D-phases during the cell cycle. This result is remarkable: subpopulations distinguished by DNA content

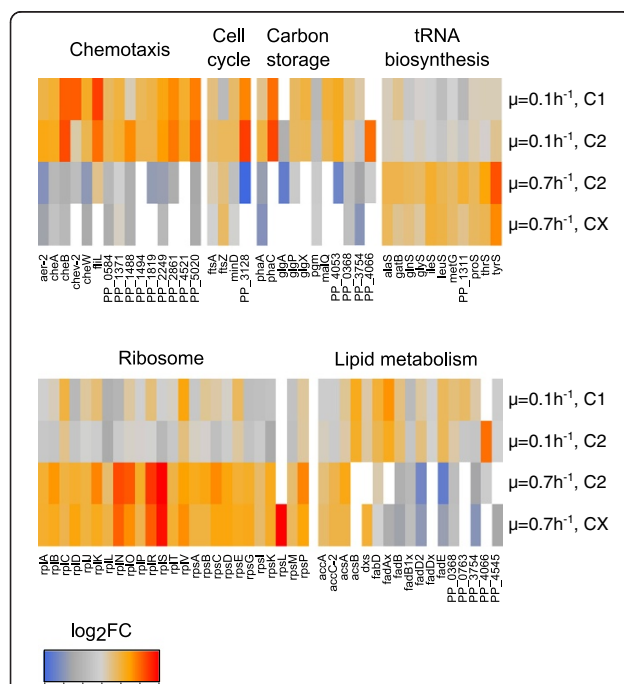


**Figure 5 Heatmaps of metabolic pathways of special interest.**

The  $\log_2$  fold changes of annotated proteins are visualized ranging from blue (low abundance) to red (high abundance). A detailed annotation of the protein names can be found in the Additional file 1. One line of the heatmap represents the different subpopulations (C1, C2 and CX) at different growth rates ( $\mu = 0.1 \text{ h}^{-1}$ ,  $\mu = 0.7 \text{ h}^{-1}$ ). Proteins of the specific pathways are shown column-wise.

appear to be physiologically highly similar provided that the growth rate is the same.

Although we are aware that subpopulations do not mirror single cell proteome compositions, the high resemblance of the subpopulations proteome patterns at the various growth rates point to their nearly identical physiological state.

One may argue whether this finding was influenced by the operation mode 'chemostat'. We identified the high similarity among subpopulations by installing distinct growth rates, because superimposing impacts in classical (fed-) batch fermentations would have prevented the unequivocal growth-to-subpopulation analysis. However, the chemostat approach might have excluded the detection of subpopulations with different protein contents because this 'growth rate filter' was installed. Assuming that cells aim to grow with the least energetic burden as possible, cellular protein compositions should be optimized at a given growth rate. Therefore, it could not be excluded, that subpopulations showing different protein patterns may have existed, but were washed-out because they could not achieve the required growth rate. While the latter demands for further in-depth analysis, the determining impact of growth on cell cycle and subpopulations is clearly visible. It gives rise to the assumption that the cell cycle itself has a minor impact on population heterogeneity under the conditions tested.

## Additional files

**Additional file 1:** Dataset of the label-free quantification (LFQ) values that were used for further analysis of differences in protein pattern.

**Additional file 2: Figure S1.** Replicate dataset of dot plots of DNA content and **Figure S2:** Overview of the total protein detection and protein annotation.

## Competing interests

The authors declare that they have no competing interests.

## Authors' contributions

SL carried out the chemostat cultivations, analysed the datasets and drafted the manuscript. MJ carried out the flow cytometry measurements, analysed the datasets and corrected the manuscript. JS and MB performed the mass spectrometry measurements. SM and RT conceived the study and corrected the manuscript. All authors read and approved the final manuscript.

## Acknowledgments

This work was supported within the ERA-IB / ERA-NET scheme of the 6th EU Framework Programme (0315932B).

## Author details

<sup>1</sup>Institute for Biochemical Engineering, University of Stuttgart, Allmandring 31, Stuttgart, Germany. <sup>2</sup>Department of Environmental Microbiology, Helmholtz Centre for Environmental Research—UFZ, Permoserstr. 15, 04318 Leipzig, Germany. <sup>3</sup>Department of Proteomics, Helmholtz Centre for Environmental Research—UFZ, Permoserstr. 15, 04318 Leipzig, Germany.

<sup>4</sup>Institute of Animal Nutrition, University of Hohenheim, Emil-Wolff-Straße 8 and 10, 70599 Stuttgart, Germany. <sup>5</sup>Department of Metabolomics, Helmholtz Centre for Environmental Research—UFZ, Permoserstr. 15, 04318 Leipzig, Germany. <sup>6</sup>Department of Biotechnology, Chemistry and Environmental Engineering, University of Aalborg, Sohngaardsholmsvej 49, 9000 Aalborg, Denmark.

Received: 18 August 2014 Accepted: 18 August 2014  
Published online: 29 August 2014

## References

- Ackermann J-U, Müller S, Lösche A, Bley T, Babel W (1995) *Methylobacterium rhodesianum* cells tend to double the DNA content under growth limitations and accumulate PHB. *J Biotechnol* 39:9–20
- Adams DW, Errington J (2009) Bacterial cell division: assembly, maintenance and disassembly of the Z ring. *Nat Rev Microbiol* 7:642–653
- Aldor IS, Keasling JD (2003) Process design for microbial plastic factories: metabolic engineering of polyhydroxyalcanoates. *Curr Opin Biotechnol* 14:475–483
- Atkinson DE, Walton GM (1967) Adenosine triphosphate conservation in metabolic regulation: rat liver citrate cleavage enzyme. *J Biol Chem* 242:3239–3241
- Avery SV (2006) Microbial cell individuality and the underlying sources of heterogeneity. *Nat Rev Microbiol* 4:577–587
- Bagdasarian M, Lurz R, Rückert B, Franklin F, Bagdasarian M, Frey J, Timmis K (1981) Specific-purpose plasmid cloning vectors II. Broad host range, high copy number, RSF 1010-derived vectors, and a host-vector system for gene cloning in *Pseudomonas*. *Gene* 16:237–247
- Blank LM, Ionidis G, Ebert BE, Bühlner B, Schmid A (2008) Metabolic response of *Pseudomonas putida* during redox biocatalysis in the presence of a second octanol phase. *FEBS J* 275:5173–5190
- Bley T (1990) State-structure models—A base for efficient control of fermentation processes. *Biotechnol Adv* 8:233–259
- Brehm-Stecher BF, Johnson EA (2004) Single-cell microbiology: tools, technologies, and applications. *Microbiol Mol Biol Rev* 68:538–559
- Bremer H, Dennis PP (1996) Modulation of chemical composition and other parameters of the cell by growth rate. *Escherichia coli* and *Salmonella*: cellular and molecular biology, vol 2, pp 1553–1569
- Buchholz A, Takors R, Wandrey C (2001) Quantification of intracellular metabolites in *Escherichia coli* K12 using liquid chromatographic-electrospray ionization tandem mass spectrometric techniques. *Anal Biochem* 295:129–137
- Carlquist M, Fernandes R, Helmark S, Heins A-L, Lundin L, Sorensen S, Gernaey K, Lantz A (2012) Physiological heterogeneities in microbial populations and implications for physical stress tolerance. *Microb Cell Fact* 11:94
- Chien A-C, Hill NS, Levin PA (2012) Cell size control in bacteria. *Curr Biol* 22:R340–R349
- Cooper S (1991) Bacterial Growth and Division: Biochemistry and Regulation of Prokaryotic and Eukaryotic Division Cycles. Academic Press, Inc, San Diego, CA
- Cox J, Mann M (2008) MaxQuant enables high peptide identification rates, individualized ppb-range mass accuracies and proteome-wide protein quantification. *Nat Biotechnol* 26:1367–1372
- Cserjan-Puschmann M, Kramer W, Duerrschmid E, Striedner G, Bayer K (1999) Metabolic approaches for the optimisation of recombinant fermentation processes. *Appl Microbiol Biotechnol* 53:43–50
- Delvigne F, Goffin P (2013) Microbial heterogeneity affects bioprocess robustness: Dynamic single-cell analysis contributes to understanding of microbial populations. *Biotechnol J* 9:61–72
- Donachie W (1968) Relationship between cell size and time of initiation of DNA replication. *Nature* 219:1077–1079
- François J, Parrou JL (2001) Reserve carbohydrates metabolism in the yeast *Saccharomyces cerevisiae*. *FEMS Microbiol Rev* 25:125–145
- Goeman JJ, van De Geer SA, van Houwelingen HC (2006) Testing against a high dimensional alternative. *J R Stat Soc Ser B (Stat Method)* 68:477–493
- Harshey RM (2003) Bacterial motility on a surface: many ways to a common goal. *Annu Rev Microbiol* 57:249–273
- Hewitt CJ, Nebe-von-Caron G, Nienow AW, McFarlane CM (1999) The use of multi-parameter flow cytometry to compare the physiological response of *Escherichia coli* W3110 to glucose limitation during batch, fed-batch and continuous culture cultivations. *J Biotechnol* 75:251–264
- Jahn M, Seifert J, Hübschmann T, von Bergen M, Harms H, Müller S (2013) Comparison of preservation methods for bacterial cells in cytomics and proteomics. *JIMICS* 3:25–33
- Jehmlich N, Hübschmann T, Gesell Salazar M, Völker U, Benndorf D, Müller S, von Bergen M, Schmidt F (2010) Advanced tool for characterization of microbial cultures by combining cytomics and proteomics. *Appl Microbiol Biotechnol* 88:575–584
- Lee JA, Spidlen J, Boyce K, Cai J, Crosbie N, Dolphin M, Furlong J, Gasparetto M, Goldberg M, Goralczyk EM, Hyun B, Jansen K, Kollmann T, Kong M, Leif R,

- McWeney S, Moloshok TD, Moore W, Nolan G, Nolan J, Nikolich-Zugich J, Parrish D, Purcell B, Qian Y, Selvaraj B, Smith C, Tchuvatkina O, Wertheimer A, Wilkinson P, Wilson C, Wood J, Zigon R, Scheuermann RH, Brinkman RR (2008) MiFlowCyt: The minimum information about a flow cytometry experiment. *Cytom Part A* 73A:926–930
- Lencastre Fernandes R, Nierychlo M, Lundin L, Pedersen AE, Puentes Tellez PE, Dutta A, Carlquist M, Bolic A, Schäpper D, Brunetti AC, Helmark S, Heins A-L, Jensen AD, Nopens I, Rottwitt K, Szita N, van Elsas JD, Nielsen PH, Martinussen J, Sørensen SJ, Lantz AE, Gernaey KV (2011) Experimental methods and modeling techniques for description of cell population heterogeneity. *Biotechnol Adv* 29:575–599
- Lindmo T (1982) Kinetics of protein and DNA synthesis studied by mathematical modelling of flow cytometric protein and DNA histograms. *Cell Tissue Kinet* 15:197–211
- Luo W, Friedman M, Shedden K, Hankenson K, Woolf P (2009) GAGE: generally applicable gene set enrichment for pathway analysis. *BMC Bioinformatics* 10:161
- Maaløe O, Kjeldgaard NO (1966) Control of macromolecular synthesis: a study of DNA, RNA, and protein synthesis in bacteria. W.A. Benjamin, Inc., New York, NY
- Martins dos Santos VAP, Heim S, Moore ERB, Strätz M, Timmis KN (2004) Insights into the genomic basis of niche specificity of *Pseudomonas putida* KT2440. *Environ Microbiol* 6:1264–1286
- Meijnen J-P, de Winde JH, Ruijsenaars HJ (2008) Engineering *Pseudomonas putida* S12 for efficient utilization of D-xylose and L-arabinose. *Appl Environ Microbiol* 74:5031–5037
- Müller S (2007) Modes of cytometric bacterial DNA pattern: A tool for pursuing growth. *Cell Proliferat* 40:621–639
- Müller S, Babel W (2003) Analysis of bacterial DNA patterns - An approach for controlling biotechnological processes. *J Microbiol Meth* 55:851–858
- Müller S, Nebe-von-Caron G (2010) Functional single-cell analyses: Flow cytometry and cell sorting of microbial populations and communities. *FEMS Microbiol Rev* 34:554–587
- Müller S, Harms H, Bley T (2010) Origin and analysis of microbial population heterogeneity in bioprocesses. *Curr Opin Biotechnol* 21:100–113
- Nahku R, Valgepea K, Lahtvee P-J, Erm S, Abner K, Adamberg K, Vilu R (2010) Specific growth rate dependent transcriptome profiling of *Escherichia coli* K12 MG1655 in accelerostat cultures. *J Biotechnol* 145:60–65
- Nakazawa T, Yokota T (1973) Benzoate metabolism in *Pseudomonas putida* (arvilla) mt-2: demonstration of two benzoate pathways. *J Bacteriol* 115:262–267
- Nelson K, Weinel C, Paulsen I, Dodson R, Hilbert H, Martins dos Santos V, Fouts D, Gill S, Pop M, Holmes M (2002) Complete genome sequence and comparative analysis of the metabolically versatile *Pseudomonas putida* KT2440. *Environ Microbiol* 4:799–808
- Neumeyer A, Hübschmann T, Müller S, Frunzke J (2013) Monitoring of population dynamics of *Corynebacterium glutamicum* by multiparameter flow cytometry. *Microp Biotechnol* 6:157–167
- Poblete-Castro I, Becker J, Dohnt K, Santos V, Wittmann C (2012) Industrial biotechnology of *Pseudomonas putida* and related species. *Appl Microbiol Biotechnol* 93:2279–2290
- Puchalka J, Oberhardt MA, Godinho M, Bielecka A, Regenhardt D, Timmis KN, Papin JA, Martins dos Santos VAP (2008) Genome-scale reconstruction and analysis of the *Pseudomonas putida* KT2440 metabolic network facilitates applications in biotechnology. *PLoS Comp Biol* 4(10):e1000210
- Rebnegger C, Graf AB, Valli M, Steiger MG, Gasser B, Maurer M, Mattanovich D (2014) In *Pichia pastoris*, growth rate regulates protein synthesis and secretion, mating and stress response. *Biotechnol J* 9:511–525
- Rønning ØW, Pettersen EO, Seglen PO (1979) Protein synthesis and protein degradation through the cell cycle of human NIH3T3 cells in vitro. *Exp Cell Res* 123:63–72
- Schaechter M, Maaløe O, Kjeldgaard N (1958) Dependency on medium and temperature of cell size and chemical composition during balanced growth of *Salmonella typhimurium*. *J Gen Microbiol* 19:592–606
- Shapiro HM (2000) Microbial analysis at the single-cell level: tasks and techniques. *J Microbiol Meth* 42:3–16
- Skarstad K, Steen HB, Boye E (1983) Cell cycle parameters of slowly growing *Escherichia coli* B/r studied by flow cytometry. *J Bacteriol* 154:656–662
- Skarstad K, Steen HB, Boye E (1985) *Escherichia coli* DNA distributions measured by flow cytometry and compared with theoretical computer simulations. *J Bacteriol* 163:661–668
- Soutourina OA, Bertin PN (2003) Regulation cascade of flagellar expression in Gram-negative bacteria. *FEMS Microbiol Rev* 27:505–523
- Spidlen J, Breuer K, Rosenberg C, Kotcheva N, Brinkman RR (2012) FlowRepository - A resource of annotated flow cytometry datasets associated with peer-reviewed publications. *Cytom Part A* 81:727–731
- Tatusov RL, Koonin EV, Lipman DJ (1997) A genomic perspective on protein families. *Science* 278:631–637
- Teather R, Collins J, Donachie W (1974) Quantal behavior of a diffusible factor which initiates septum formation at potential division sites in *Escherichia coli*. *J Bacteriol* 118:407–413
- Theobald U, Mailinger W, Baltes M, Rizzi M, Reuss M (1997) In vivo analysis of metabolic dynamics in *Saccharomyces cerevisiae*: I. Experimental observations. *Biotechnol Bioeng* 55:305–316
- Unthan S, Grünberger A, van Ooyen J, Gätgens J, Heinrich J, Paczia N, Wiechert W, Kohlheyer D, Noack S (2014) Beyond growth rate 0.6: What drives *Corynebacterium glutamicum* to higher growth rates in defined medium. *Biotechnol Bioeng* 111:359–371
- Weart R, Lee A, Chien A-C, Haeusser D, Hill N, Levin P (2007) A metabolic sensor governing cell size in bacteria. *Cell* 130:335–347
- Yuste L, Hervás AB, Canosa I, Tobes R, Jiménez JL, Nogales J, Pérez-Pérez MM, Santero E, Díaz E, Ramos JL, De Lorenzo V, Rojo F (2006) Growth phase-dependent expression of the *Pseudomonas putida* KT2440 transcriptional machinery analysed with a genome-wide DNA microarray. *Environ Microbiol* 8:165–177

doi:10.1186/s13568-014-0071-6

**Cite this article as:** Lieder et al.: Subpopulation-proteomics reveal growth rate, but not cell cycling, as a major impact on protein composition in *Pseudomonas putida* KT2440. *AMB Express* 2014 4:71.

**Submit your manuscript to a SpringerOpen® journal and benefit from:**

- Convenient online submission
- Rigorous peer review
- Immediate publication on acceptance
- Open access: articles freely available online
- High visibility within the field
- Retaining the copyright to your article

Submit your next manuscript at ► [springeropen.com](http://springeropen.com)